Ytterbium(III) Complex with Photochromic Ruthenium(II) Acetylide Ligand: All Visible Light Photoswitching of NIR Luminescence

Pramila Selvanathan, Elsa Tufenkjian, Olivier Galangau, Thierry Roisnel, François Riobé, Olivier Maury, Lucie Norel, Stéphane Rigaut

Ytterbium(III) complex with photochromic ruthenium(II) acetylide ligand: all visible light photoswitching of NIR luminescence

Pramila Selvanathan,[†] Elsa Tufenkjian,[†] Olivier Galangau,[†] Thierry Roisnel,[†] François Riobé,[‡] Olivier Maury,[‡] Lucie Norel,*[†] Stéphane Rigaut*[†]

[†] Univ Rennes, CNRS, ISCR (Institut des Sciences Chimiques de Rennes) – UMR 6226, F-35000 Rennes, France.

[‡] Univ. Lyon, CNRS, Ecole Normale Supérieure de Lyon, Laboratoire de Chimie UMR 5182 46 allée d'Italie, F-69007 Lyon, France.

Corresponding author e-mails : lucie.norel@univ-rennes1.fr, stephane.rigaut@univ-rennes1.fr

ABSTRACT: We report a ruthenium(II) bisacetylide complex bearing a photochromic dithienylethene (DTE) acetylide arm and a coordinating bipyridyl on the trans acetylide unit. Its coordination with Yb(TTA)$_3$ centers (TTA = 2-thenoyltrifluoroacetonate) produces a bimetallic complex in which the dithienylethene isomerization is triggered by both UV light absorbed by the DTE unit and 450 nm excitation in the transition of the organometallic moiety. The redox behavior arising from the ruthenium(II) bisacetylide system is fully investigated by cyclic voltammetry and spectroelectrochemistry revealing a lack of stability of the DTE closed oxidized state preventing effective redox luminescence switching. On the other hand, the photoswitching of ytterbium(III) NIR emission triggered by the photochromic reaction is fully operational. The electronic structure of this complex in its different states characterized by strong electronic coupling between the DTE and the ruthenium(II) based moieties leading to metal assisted photochromic behavior were rationalize with the help of TD-DFT calculations.

INTRODUCTION

The conception of all-optical materials featuring photocontrol of the light emitted from a molecular system at will is a key achievement of the field of molecular materials.[1-6] The versatility of molecular design allows the selection of various specific characteristics and such photoswitchable emissive molecules already found applications in the field of bioimaging,[7] anticounterfeiting,[8] sensors[9] and so on.[10-12] In this context, it is particularly appealing to exploit the specific emission signatures of 4f metal complexes owing to their large pseudo-Stokes shifts, narrow bandwidth emission bands and long emission lifetimes.[13-14] The optical switching of lanthanide emission with organic photochromic units has been mainly achieved with dithienylethene (DTE),[4] or closely related structures,[15] and is based on a large conjugation change upon a reversible photoreaction between the two photoisomers. To that regard, the literature is almost entirely focused on red emissive europium(III) coordination complexes,[15-28] which involve in most cases the photocontrol of a resonant energy transfer between the emissive ion and the photochromic unit in the more conjugated closed form featuring a large and intense absorption bands at 500-600 nm not observed with the open isomer. However, one particularly interesting feature of 4f metal complexes is the accessibility of pure near infrared (NIR) response, for instance with ytterbium(III) centers, at wavelengths close to 1000 nm relevant for both material science and biology.[29] This has been a strong motivation for us to investigate the design of efficient ytterbium based emission photoswitches, identify the effective mechanisms allowing a DTE unit to perturb emission in this wavelength range, and target the optimization of the optical response parameters (contrast, brightness, time response).

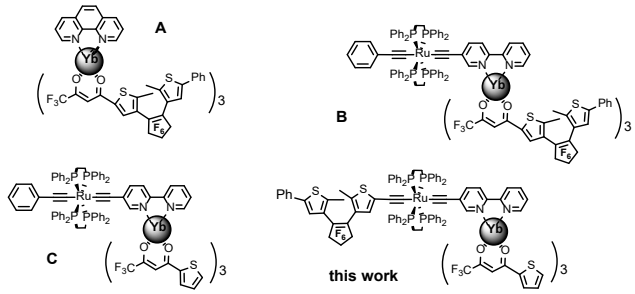

Chart 1. Previously investigated ytterbium(III) luminescence switches relevant for the present study.

We recently reported an efficient example using a DTE appended β-diketonate ligand as photoswitching unit (complex **A** in chart 1) displaying a dynamic emission response.[30] Indeed, when excitation was performed at the photocyclization wavelength (λ = 350 nm), a fast decrease of the emission (down to 1.4 % of initial maximum intensity) along with blue coloration were observed. Then, total recovery of the emission and discoloration was obtained upon visible light irradiation due to cycloreversion. In parallel to that work, combination with a redox active ruthenium bis(acetylide) moiety (complex **B**, chart 1) allowed additional features to be implemented. First, redox switching of emission was obtained, in line with our previous results on complex **C**.[31] Second, the photocontrol of a static luminescence process with the use of the metal-to-ligand charge transfer (MLCT) transition to sensitize the ytterbium(III) ion without inducing any photochromic reaction provided nondestructive readout.[32] At this stage, the question of the generality of ytterbium emission switching with DTE units arises as well as the possibility that alternative photochromic ligand designs

could produce different responses. To that regard, it is interesting to note that a DTE appended cyclen complex of ytterbium(III) shows in contrast a non-emissive behavior at room temperature.[33] With this in mind, we describe in the following another design for NIR luminescence photocontrol of ytterbium(III) emission in which the DTE unit is inserted as an acetylide ligand of the ruthenium center, thus leading to stronger electronic coupling between the photochromic unit and the redox active moiety (Scheme 1). Our study shows that this new design is also efficient in producing NIR photocontrol and that DTE appended β-diketonate ligands are not necessarily required. This new design features efficient closing reaction leading to the quenching of ytterbium(III) emission that can be triggered as expected by UV light (350 nm) but also by blue light (450 nm). To that regard, TD-DFT investigations evidence a high degree of orbital mixing between the DTE and ruthenium bis(acetylide) moiety and explain why this new fast MLCT induced closing of the DTE unit is experimentally observed.[34-38] This detailed study featuring electrochemistry, spectroelectrochemistry, photochromism and luminescence studies, as well a theoretical calculations provides a guide for further rationalization and subsequent designs of photo- or dual switches pointing key design elements.

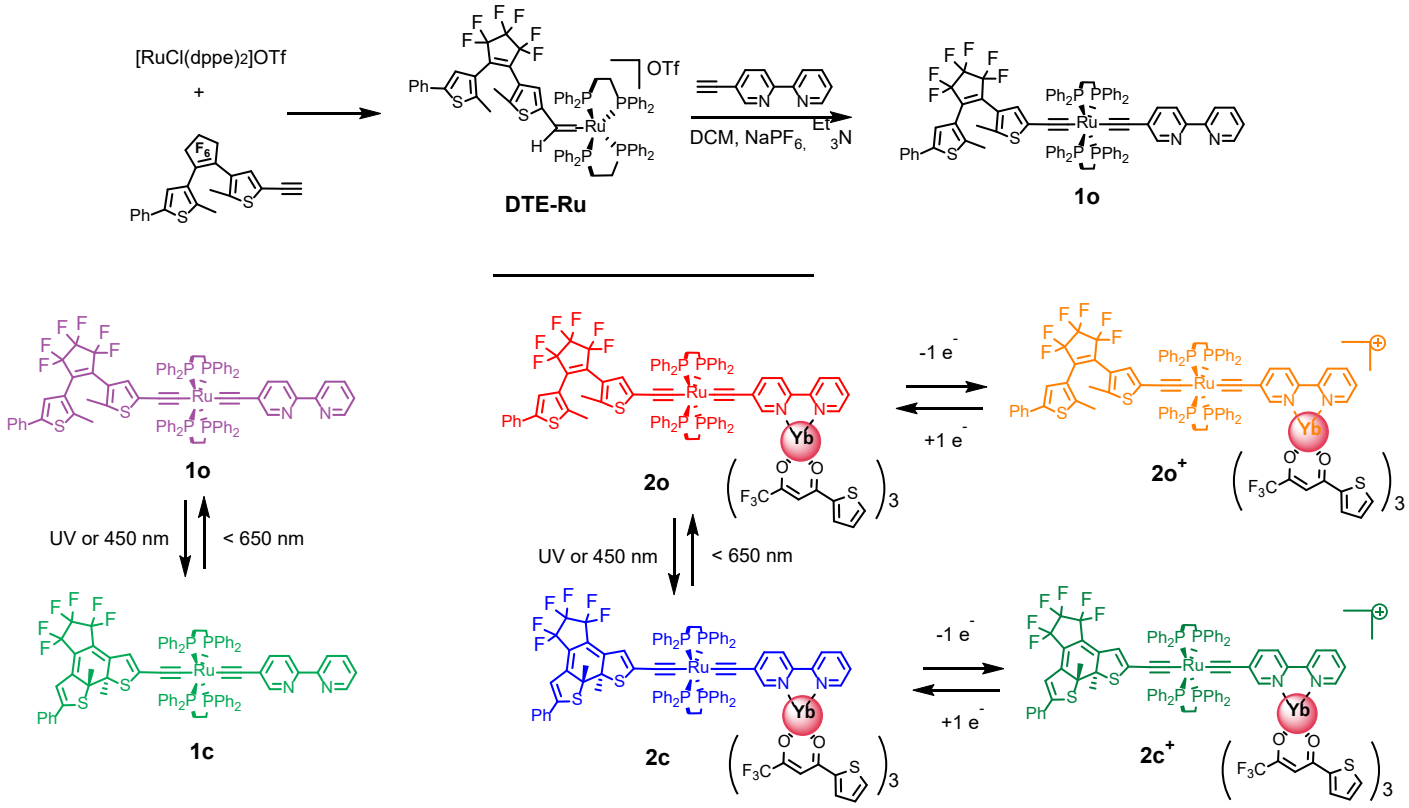

Scheme 1. Final steps of the synthesis of complex 1o (top) and the different states of ligand 1o and bimetallic complex 2o due to (i) photoisomerization of the DTE and (ii) oxidation/reduction of the ruthenium bis(acetylide) moiety (bottom).

RESULTS AND DISCUSSION

Complex synthesis. The organometallic ligand was synthesized according to the classical procedure for ruthenium bis-acetylide complexes (Scheme 1). First, the vinylidene complex [Ph-DTE-CH=C=Ru(dppe)$_2$Cl](OTf) (**DTE-Ru**) was prepared from the corresponding free alkyne[39] and the 16 electrons complex [Cl-Ru(dppe)$_2$](OTf). Then, the second acetylide ligand was introduced by reacting 5-ethynyl-2,2'-bipyridine[40] with **DTE-Ru** in presence of triethylamine and $NaPF_6$, to form complex [Ph-DTE-C≡C-(dppe)$_2$Ru-C≡C-bpy] (**1o**). Finally, [Yb(TTA)$_3$(H$_2$O)$_2$] was reacted with **1o** at room temperature in dichloromethane to yield the bimetallic complex **2o**. The compounds were also fully characterized by NMR, EA and HRMS with classical characteristic features (see ESI). For both **1o** and **2o**, crystallization by layering a dichloromethane solution of the compound with pentane and slow mixing of the layers resulted in crystals suitable for single crystal XRD study. However, in both cases, the quality of the final refinement is quite poor with R factors values of 0.1396 (for **1o**) and 0.1857 (for **2o**). Therefore, this data do not provide reliable metrics for the two structures and has been solely used as complementary evidence of the nature of the two complexes (see ESI).

Absorption spectroscopy and photoisomerization. The UV-visible spectra in dichloromethane have been measured for both **1o** and **2o** as shown in Figures 1 and 2. For **1o**, the energy band observed at 394 nm is characteristic of the ruthenium acetylide moiety, usually described as multiconfigurational MLCT excitations corresponding to transitions from Ru(dπ)/alkynyl-based orbitals to metal/ligand antibonding orbitals combined with intra ligand π → π* character.[41] For **2o**, two main absorption bands at λ_{max} = 338 nm (59 000 L.mol^{-1}.cm^{-1}) and at λ_{max} = 454 nm (16 000 L.mol^{-1}.cm^{-1}) are observed. The band at 338 nm is assigned to the TTA ligand absorption by comparison with [Yb(TTA)$_3$·2H$_2$O] precursor, probably overlapping with transitions of π–π* character centered on the bipyridyl and DTE moieties. The band at 454 nm corresponds to the aforementioned MLCT transition, bathochromically shifted as compared with

1o (ΔE_{max} = 3355 cm^{-1}) because of the enhanced accepting ability of the bpy unit upon complexation with ytterbium.[31, 42-43] As a result, decoordination

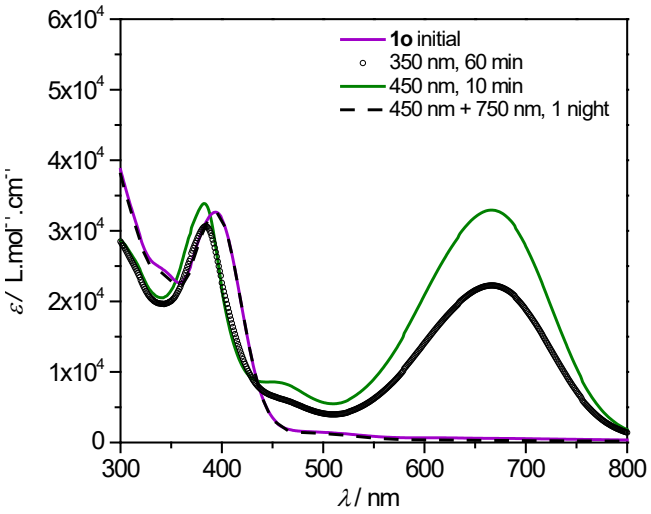

Figure 1. Electronic absorption spectra of complex **1o** in dichloromethane (2.70 10^{-5} M) and of the PSS obtained after 450 nm irradiation. The spectrum obtained after 350 nm irradiation is shown for comparison. Complete color fading is observed upon 750 nm irradiation in both cases.

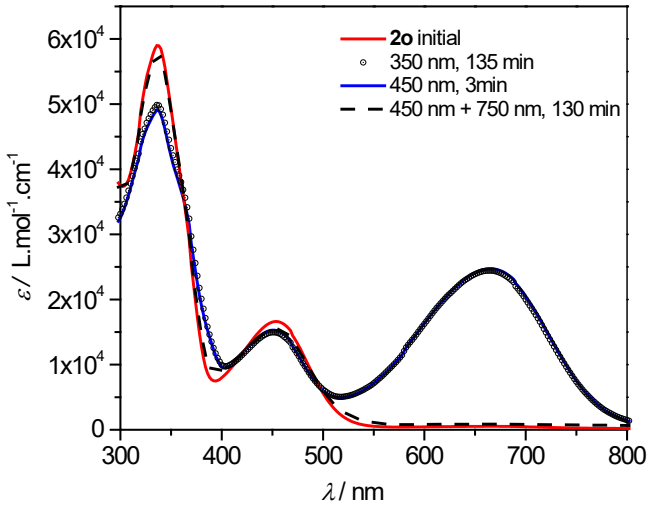

Figure 2. Electronic absorption spectra of complex **2o** in dichloromethane (1.19 10^{-5} M) and of the PSS obtained after 350 nm or 450 nm irradiation. Complete color fading is observed upon 650 nm irradiation in both cases.

When the solutions of **1o** and **2o** were irradiated with UV light (λ = 350 nm), they both developed an intense blue color due to photoisomerization of the DTE unit. More precisely, for **1o**, the band at λ_{max} = 394 nm was slightly shifted to higher energies, while a broad band centered at λ_{max} = 666 nm appeared, which is usually assigned to the closed DTE π–π* transition in **1c**. The photostationary state (PSS) was completed after 60 minutes in the experimental conditions ([c] = 2.7×10^{-5} mol.L^{-1}). For **2o**, while the band at λ_{max} = 338 nm decreased, the MLCT transition remained unaffected and a new broad band was observed at λ_{max} = 666 nm. The closing of the DTE moiety to form **2c** was completed after 135 minutes in the experimental conditions ([c] = 1.19×10^{-5} mol.L^{-1}). Both compounds showed complete color fading and recovery of 99 % of the intensities of the initial spectra upon further irradiation in the closed DTE π–π* transitions (either at λ = 650 nm or at λ = 750 nm). The comparison of the behavior of the two compounds gives some insights on their electronic structures: it is striking to observe that the low energy DTE bands in **1c** and **2c** overlap, pointing to a transition centered on the DTE acetylide, with a negligible participation from the rest of the organometallic ligand.

We also investigated the possibility of sensitized photoisomerization by selective irradiation in the MLCT band of **2o**. Upon irradiation at λ = 450 nm, photoisomerization indeed occurred, and the reaching of an identical PSS state to that observed at 350 nm was much faster (3 vs. 135 minutes), in part due to the higher irradiation power at 450 nm (0.6 mW at 350 nm, 3 mW at 450 nm). Experimentally, the quicker closing at 450 nm is advantageous for limiting light exposure and possible bleaching of the compound upon long exposures to UV light. In the case of **1o**, we observed that 450 nm also lead to fast closing with a higher photoconversion at this wavelength as compared with 350 nm (Figure 1).

Table 1: Main transitions observed in the electronic absorption spectra of 1 and 2 in their different states

	λ_{max} **(nm)** [ε ($L.mol^{-1}.cm^{-1}$)]		
1o	**394** [32000][a]		
1c	**382** [34000][a]	**666** [33000][a]	
1o$^+$	**378** [19000][b]		**1197** [9000][b]
1c$^+$	**348** [31000][b]	**654** [25000][b]	**949** [11000][b]
2o	**454** [16000][a]		
2c	**451** [15000][a]	**666** [25000][a]	
2o$^+$	**442** [13000][b]		**1167** [5600][b]
2c$^+$	**394** [31000][b]	**648** [13000][b]	**943** [8300][b]

a measured in dichloromethane (see Figures 1 and 2), b measured in an OTTLE cell, with 0.2 M NBu4PF6 in dichloroethane (see Figures 4 and S10).

In parallel, to determine the PSS compositions, we first performed NMR monitoring of the isomerization process (λ = 450 nm, $CDCl_3$) on **1o**. In the ^{31}P NMR spectra, the characteristic resonance of the four equivalent phosphorous atoms are shifted from 53.3 ppm in **1o** to 52.4 ppm in **1c** (Figure S6), while in the ^1H NMR spectra, characteristic shielding of the thiophene protons and deshielding of the methyl protons are observed upon closing of the system (Figure S4-5). A PSS composition of 95 % of **1c** was determined by integration of these different signals. Then, the full reversibility of the process was observed after 650 nm irradiation. Due to the strong paramagnetism of **2o**, it was difficult to obtain informative NMR spectra at low concentration (necessary for photoisomerization) and we determined the PSS composition by titration of **1c** by $[Yb(TTA)_3(H_2O)_2]$. More specifically, a dilute solution of **1c** (PSS) was titrated with a solution of $[Yb(TTA)_3(H_2O)_2]$ following the expected shift of the MLCT transition occurring upon complexation (Figure S7). When no further changes were detected because of complete coordination, the spectrum was compared to the PSS obtained from irradiation of **2o** and we concluded that the photoconversion was similar to that of **1c** (ca. 95 % of **2c** at the PSS).

Computational study. TD-DFT calculations (see SI for details) were performed to confirm the above mentioned assignments and allow to better describe the nature of each electronic transition. For **1o**, the X-Ray structure was used as input for geometry optimization. The HOMO was calculated at -4.79 eV and is developed as expected on the ruthenium atom, alkynyl thiophene and alkynyl bipyridine moieties. The LUMO orbital is developed only on the DTE moiety and shows the expected bonding character between the reactive carbon atoms of the thiophene rings, explaining why transitions implying this orbital could induce the electrocyclic closing reaction of the DTE unit as illustrated bellow. This is the case of several charge transfer transitions with low oscillator strength calculated between 400 and 600 nm with a predominant contribution from a HOMO-n →LUMO (with n= 0, 1,2) transition (*vide infra*). However, the more intense transitions of the calculated spectrum (at λ_{theo} = 425 nm) involving the HOMO and the LUMO+1 or LUMO+2, the latter being centered on the DTE or bipyridine (π*), are not photochromic. Note that the overall spectrum is in reasonable agreement with the experimental one but globally red-shifted so that this last transition is found experimentally at 394 nm.

For **2o**, Yb was replaced by Y in a model compound for minimizing calculation cost.[44] The nature of the HOMO is similar to the one of **1o** and calculated at -4.92 eV. The LUMO+n (n= 0, 1, 2) are very close in energy and located mainly on the TTA ligands with some contribution on the bipyridine unit. The initial LUMO in **1o** splits into two close lying LUMO+3 and LUMO+4 in **2o** that can also lead to photoisomerization. Additionally, these virtual orbitals feature density developing onto the TTA / bipyridine fragments (see Figure S25-26). The calculated absorption spectrum reveals a large degree of mixing between the different orbitals in the calculated transitions which ultimately lead to two bands. The first band, predicted at 500 nm and measured at 454 nm, entails several components with a d/π → LUMO+n (n= 0, 1, 2, 3, 4) character and thus could be qualified as MLCT / ML'CT with multiconfigurational transitions involving both the bpy and tta moieties as acceptors. Interestingly, calculations indicate in transitions n° 2, 3, 6, 7 and 8 a significant contribution of the LUMO+3 and the LUMO+4, which can be described as intrinsically photochromic. Therefore, the resulting MLCT absorption band in **2o** endows a photochromic character leading to the cyclization of the diarylethene fragment. These conclusions can be extended to the second band at higher energy (at λ_{theo} = 380 nm), calculated as an overlap of several transitions, including photochromic ones with contributions from various orbitals.

In line with our experimental observations, the calculations on the close isomer **1c** predict a quite pure (92 %) HOMO to LUMO transition at 671 nm with the expected π–π* character centered on the DTE alkyne arm, and to a lesser extent on the ruthenium atom. For **2c**, the low energy transition has the same nature (98 % HOMO to LUMO) and is calculated at 666 nm. Also note that the MLCT transitions show a slight hypsochromic shift upon photoisomerization, of **1o** to **1c** (ΔE_{max} = -cm^{-1}). This is consistent with a main charge transfer of the type Ru(dπ)/alkynyl-based orbital to the bipyridine/DTE(π*) one operating in **1o** switching to a Ru(dπ)/alkynyl → bipyridine (π*) in **1c**. On the contrary, after ytterbium coordination, almost no change of the MLCT position upon isomerization from **2o** to **2c** (ΔE_{max} = -191 cm^{-1}) is observed, but the high degree of mixing of different orbitals and the presence of different transitions in this region makes any further interpretation difficult.

To conclude this part, although the MLCT sensitized isomerization reaction reported here is experimentally similar to the one of platinum sensitized diarylethene described by Branda et al., our calculations indicate some important distinctive features. In Branda's work, the mechanism consist in a transfer from the ^{3}MLCT state to a DTE centered ^{3}IL that evolves towards the closed isomer and the conjugation between the DTE and the organometallic unit governs the transfer efficiency.[36-37] Our computations, which takes into account only singlet states, would indicate that the observed photochromic character is inherent to the strong electronic coupling between the DTE, the 4d metal and the bipyridine fragment within compound **2o**. This creates multiple excited states with density developing on both the DTE and the 4d center that can explain visible light triggered photochromism without relying on triplet states.

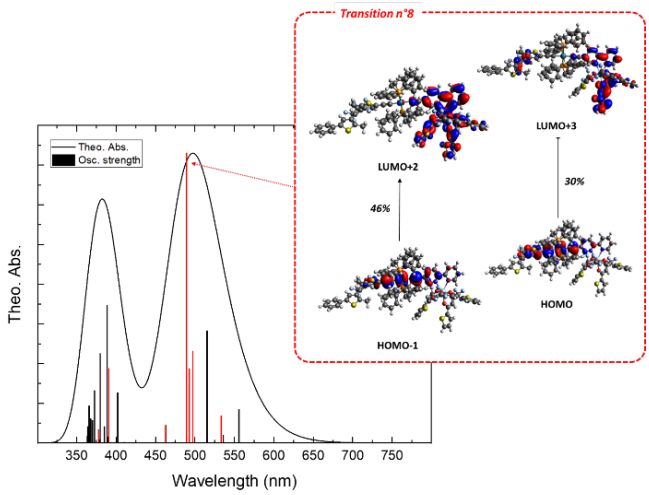

Figure 3. Theoretical Absorption spectrum of **2o.** Photochromic transitions are highlighted in red. Transition n°8 was chosen to illustrate the nature of the vertical transitions, displaying 4d/π – 4f or π* character.

Electrochemical and spectroelectrochemical behaviors. The electrochemical behavior of complexes **1o** and **2o** was studied by cyclic voltametry (see ESI for details). Compound **1o** undergoes a one-electron reversible oxidation process at E_1° = 0.055 V versus $FeCp_2/FeCp_2^+$ (ΔEp = 58 mV), as expected for such an organometallic ruthenium based moiety, followed by a partially irreversible process. For **2o**, the one-electron reversible oxidation was observed at E_1° = 0.077 V (ΔEp = 63 mV). The comparison between **1o** and **2o** is consistent with the HOMO of the complex being stabilized upon complexation, as in the calculation (stabilization of ca. 0.100 eV (vide supra)). As expected, the oxidation potential was modified upon photoisomerization with a lower oxidation potential of 0.013 V for **2c.** Actually, in **2o** the HOMO is delocalized over the acetylide fragment including some 4d orbital contribution while in **2c** the HOMO is mainly DTE centered leading to a destabilization by 70 meV upon the closing reaction, exactly in line with the experimental value (65 meV).

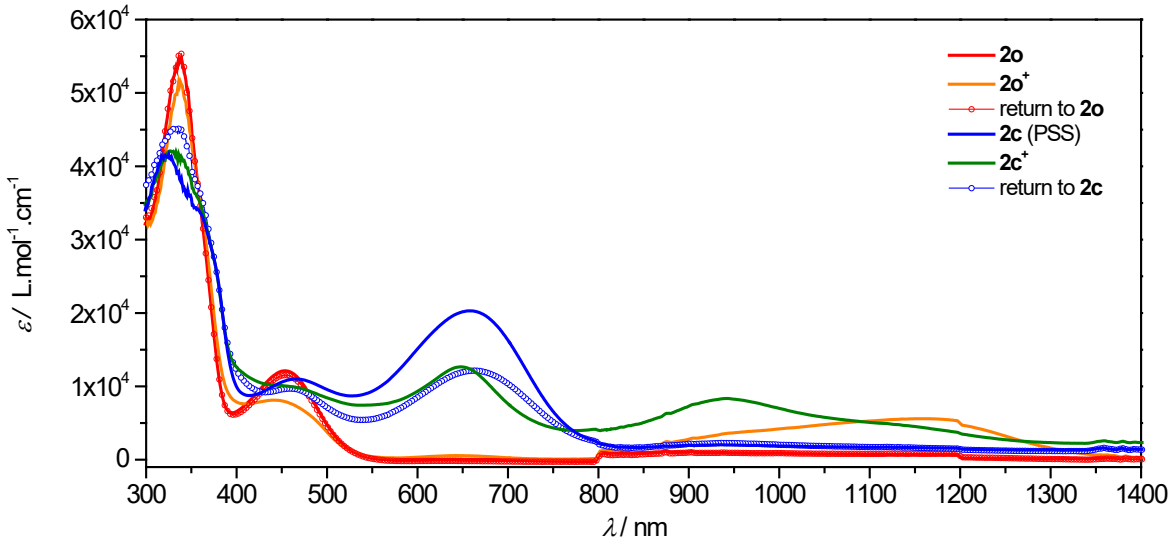

Figure 4. UV-vis-NIR spectra of **2o** (resp. **2c**) upon oxidation to **2o**$^+$ (resp **2c** $^+$) in degassed dichloroethane (0.2 M NBu_4PF_6). **2o**$^+$ was generated by application of a positive potential, then the reduction to **2o** was achieved at 0V. **2c** was obtained *in situ* upon 450 nm irradiation for 15 min. **2c**$^+$ was generated by application of a positive potential, then partial return to **2c** was obtained at 0V.

We further performed UV-vis-NIR absorption spectroscopies in an optically transparent thin-layer electrochemical (OTTLE) cell to characterize the first oxidations states with the aim to achieve redox luminescence switching. Upon oxidation of **1o** to **1o**$^+$, the MLCT band at 394 nm decreased while a new broad band increased, from ca. 850 nm to 1400 nm (λ_{max} = 1197 nm), with probably LMCT and LLCT characters (Figure S10). This large NIR absorption band is typical of such ruthenium acetylide systems[45-46] and has previously been ascribed to a SOMO-n to SOMO transition mainly delocalized over the carbon rich path in related complexes.[41] These changes were reversible upon reduction. A similar experiment was carried out on **1c** obtained by *in situ* irradiation. Upon oxidation to **1c**$^+$, the vanishing of the MLCT band at 382 nm was observed and bands centered on the DTE were also clearly affected with a decrease of the transition centered at 670 nm while a new broad band from ca. 800 nm to 1300 nm increased, which is shifted to λ_{max} = 949 nm as compared with **1o**$^+$ (λ_{max} = 1197 nm). Importantly, the perturbation of the transition at 670 nm is consistent with the HOMO of **1c** being delocalized on the DTE alkyne arm

The same experiment was then performed on **2o** (Figure 4). The observed changes upon oxidation to **2o**$^+$, ie the decrease of the band at λ_{max} = 455 nm and a new broad absorption band in the NIR region of the spectrum with λ_{max} = 1167 nm are very similar to the one observed for the monometallic complex **1o**. The NIR band is also similar but red-shifted, compared to the parent complex **A** (λ_{max} = 1060 nm) which does not bear the DTE alkyne arm. For the closed compound **2c**, the behavior seems to be very similar to the one of **1c**, but the reversibility of the process was very poor indicating degradation of the closed bimetallic complex. Therefore, at this stage, even if we can foresee that oxidation to **2o**$^+$ would probably lead to a non-emissive state due to the presence of low energy electronic transitions in in the range of ytterbium(III) emission,[31] the lack of stability of **2c**$^+$ prevents the achievement of a reversible redox switch. Indeed sensitization of the ytterbium(III) ion would lead to concomitant closing whatever the excitation wavelength and to the appearance of unstable **2c**$^+$.[45]

Emission studies. In the previously investigated complex B (Scheme 1), the low energy transition at 450 nm could be used to sensitize the ytterbium centered emission in the NIR region without any photoisomerization of the DTE unit, thus providing a way for non-destructive readout of the system emission. In the case of **2o,** all possible sensitization wavelengths lead to the closing of the DTE and the excitation light for luminescence induces at the same time the desired emission and the isomerization. Therefore, in the present case, the emission response always corresponds to a dynamic evolving system. For the reason mentioned above, we decided to focus on the emission intensity evolution of **2o** upon photocyclisation to **2c** only, and discard the redox commutation due to the unstablility of **2c**$^+$. The spectra were measured on stirred dichloromethane solutions at room temperature. Note that no emission was detected in the visible range at room temperature.

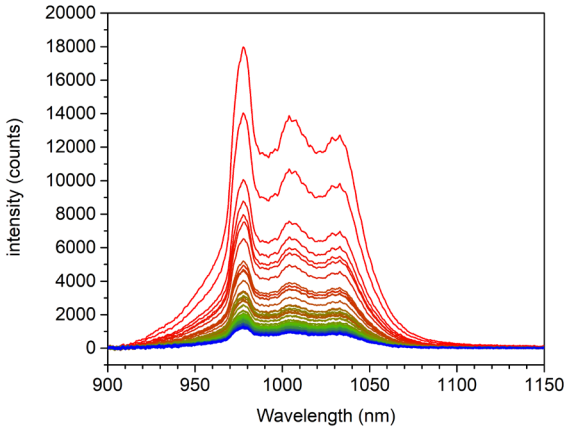

Figure 5. Room temperature emission spectra of **2o** (evolving to **2c**) upon continuous excitation at 450 nm until the PSS was reached (1.3 s delay between successive spectra).

Monitoring the NIR response of **2o** with a CCD detector allows a fast and simultaneous acquisition of the entire wavelength range upon excitation at 338 nm (Figure S11) or at 450 nm in the MLCT transition of the acetylide moiety (Figure 5). It reveals the typical signature of ytterbium(III) centered luminescence originating from the $^2F_{5/2} \rightarrow {}^2F_{7/2}$ transition. The spectrum is dominated by the sharp zero-phonon line at 978 nm and structured with two additional bands at 1005 nm et 1032 nm. Thussensitization occurs in both excitation ranges.

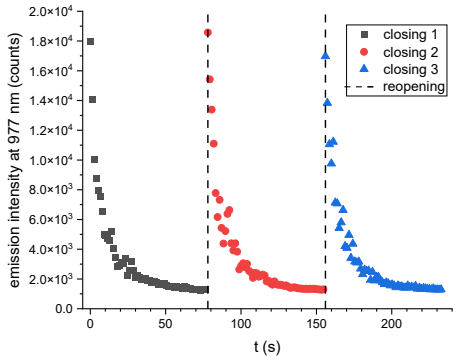

Figure 6. Monitoring of emission intensity (λ_{em} = 977 nm) of **2o** (evolving to **2c**) upon continuous excitation at 450 nm. Reopening was performed in the spectrometer with 662 nm irradiation.

Quite rapidly upon 450 nm (Figure 5) and 338 nm (Figure S11) excitation, the emission response fades with time and the final spectrum corresponds to an integrated area of 7 % and 13 %, respectively, of the initial spectrum. Importantly, the absorption of the final solution also matches the one of **2c** at the PSS demonstrating the expected conversion in these conditions. We can therefore conclude that the closing of the DTE causes a very efficient quenching of the system luminescence with a remaining intensity quite consistent with the presence of ca 5% of open state (*vide supra*). The initial luminescence was recovered upon 662 nm irradiation performed in the fluorimeter in order to switch the system back to its open state and three successive closing could be performed with similar quenching efficiencies (Figure 6 and S11).Finally, upon excitation at 662 nm of **2c**, no NIR emission was obtained. Like the previously reported systems A and B, **2c** shows no absorption in the NIR range and unlike for europium complexes, FRET energy transfer with the closed DTE playing the role of the acceptor cannot explain the quenching. We thus tentatively assign this effect to a low lying and non-emissive triplet state centered on the closed DTE unit that operates to quench the luminescence.

This is overall the third example of a DTE unit that is efficient at switching ON and OFF ytterbium emission,[33] with a different design and still a very high intensity quenching ratio. The best system in term of ON/OFF emission contrast has been obtained for complex B[32] and the related monometallic complex A[30] with residual intensity in the closed state lower than 2% of the initial one. Note however that such complexes bear three photoswitches per ytterbium, instead of one in the present case, rendering the quenching more efficient at any given photoconversion. Finally, the design presented here, with the DTE participating in the conjugated system of a ruthenium bisacetylide, presents the additional feature of being controllable at 450 nm, at lower and less harmfull energy than previously reported systems.

CONCLUSION

In this study, we have combined an emissive ytterbium(III) center with a photochromic ruthenium bisacetylide moiety to generate a light and redox sensitive bimetallic complex with a new design. The high degree of electronic coupling between the diarylethene moiety and the rest of the ruthenium bisacetylide, also evidenced through DFT calculations, leads to visible light induced isomerization reaction not observed in the other parent complexes. Therefore, the ytterbium centered NIR emission can be switched ON and OFF with visible light only, ie. using 450 nm and 662 nm irradiation wavelengths, therefore allowing the use of low energy excitations in both directions. With the present results, we demonstrate that the control of NIR emission with DTEs is a rather general feature of this family of photoswitches. Our future efforts will be directed at identifying the mechanism of the quenching and the possible involvement of dark triplet states of the DTE closed isomers funneling away the energy of Yb excited state.

EXPERIMENTAL SECTION

General comments. The reactions were carried out under an argon atmosphere using Schlenk techniques. Solvents were dried and distilled using standard procedures. ^{1}H and ^{13}C NMR spectra were recorded at 303 K on a Bruker III Avance 400 MHz or on a Bruker Avance III HD 500 MHz at the Centre Régional de Mesures Physiques de l'Ouest. IR experiments were performed on an IRAffinity-1 (CSHIMAD20) spectrometer on the bulk material. High resolution mass spectra were recorded on a Thermo Fisher Scientific Q-exactive instrument working under positive electrospray ionization mode at the Centre Régional de Mesures Physiques de l'Ouest. Elemental analysis were obtained on a Perkin Elmer 2400 Series II combustion analyser at the UC Berkeley College of Chemistry Microanalytical Facility or a Flash 1112 Thermo Fischer analyser at the Centre Régional de Mesures Physiques de l'Ouest. Details of the spectroscopic measurments can be found in the SI. Degassed solvents were used only in the case of spectroelectrochemical measurements.

[Ph-DTE-CH=C=Ru(dppe)$_2$Cl](OTf) DTE-Ru. In a Schlenk tube, Ph-DTE-≡-H[39] (162.1 mg, 0.34 mmol, 1.2 eq) and [Cl-Ru(dppe)$_2$](OTf) (310 mg, 0.28 mmol, 1 eq) were dried under vacuum for 30 minutes. Then, degassed dichloromethane (14 mL) was added to the Schlenk tube and the reaction mixture was stirred for 2 days at room temperature. Precipitation was achieved with addition of a 1:2 dichloromethane and pentane mixture to yield the compound **DTE-Ru** (446 mg, 92 %). ^{1}H NMR ($CDCl_3$, 400 MHz): δ (ppm) = 1.67 (s, 3H, Me), 1.89 (s, 3H, Me), 2.75 (bs, 4H, $P(CH_2)_2P$), 2.90 (bs, 4H, $P(CH_2)_2P$), 4.57 (s, 1H, H_b), 5.56 (s, 1H, H_{Th}), 7.02 (s, 1H, H_{Th}), 7.08-7.13 (m, 14H, H_{ar}), 7.23-7.29 (m, 17 H, H_{ar}), 7.31-7.7.40 (m, 12H, H_{ar}), 7.47-7.49 (m, 2H, H_{ar}). ^{31}P NMR ($CDCl_3$, 400 MHz): δ (ppm) = 37.8 (s, 4P).

***trans*-[Ph-DTE-C≡C-(dppe)$_2$Ru-C≡C-bipy] 1o.** In a Schlenk tube, **DTE-Ru** (400 mg, 0.286 mmol), $NaPF_6$ (97 mg, 0.57 mmol), and 5-ethynyl-2,2'-bipyridine[40] (51.82 mg, 0.286 mmol) were dried under vacuum for 30 min. Then, dichloromethane (56 mL) mixed with triethylamine (1.6 mL) was saturated with argon, and transferred into the Schlenk tube. The mixture was stirred at room temperature for 18 h, and the solution was filtered and taken to dryness under vacuum. The residue was redissolved in CH_2Cl_2 (10 mL) and the precipitation

was completed by the addition of MeOH (15 mL). The compound was further recrystallized from 1:2 CH_2Cl_2/pentane to yield green crystals (398 mg, 90 %). ^{1}H NMR ($CDCl_3$, 400 MHz): δ (ppm) = 1.87 (s, 3H, $Me_{1'}$), 1.99 (s, 3H, Me_1), 2.64 (s, 8H, $P(CH_2)_2P$), 6.28 (s, 1H, $H_{2'}$), 6.98-7.06 (m, 17H, H_4 and m-PPh2), 7.19-7.22 (m, 9H, $H_{5'}$ and p-PPh2), 7.31 (m, 3H, H_2 and C6H5-DTE), 7.36-7.38 (m, 10H, C_6H_5-DTE and o-PPh_2), 7.55-7.59 (m, 9H, C_6H_5-DTE and o-PPh_2), 7.81 (t, J = 6.9 Hz, 1H, $H_{4'}$), 8.14 (d, J = 8.5 Hz, 1H, H_3), 8.19 (s, 1H, H_6), 8.35 (d, J= 7.8 Hz, 1H, $H_{3'}$), 8.70 (d, J = 3.6 Hz, 1H, $H_{6'}$). ^{31}P NMR ($CDCl_3$, 400 MHz): δ (ppm) = 53.3 (s, 4P). ^{13}C NMR ($CDCl_3$, 400 MHz): δ (ppm) = 156.75 (C_{bpy}), 150.28 (C_6), 149.69 (C_{bpy}), 149.13 ($C_{6'}$), 141.87 (C-Me_1), 141.13 (C_q), 137.47 (C_4), 136.74 ($C_{4'}$), 136.7 (m, ipso-PPh2), 136.50, 134.23 (o-PPh2), 133.91 (o-PPh2), 133.49 (C_q), 129.70 (C_q), 129.01(p-PPh2), 128.74 (p-PPh2), 127.81 (CH), 127.18 (m-PPh2), 126.37 (**C**-C_5F_8), 125.58 (CH), 124.01 (**C**-$H_{2'}$), 123.87 (**C**-C_5F_8), 122.69 (**C**-H_2), 120.69 ($C_{3'}$), 120.04 (C_3), 119.42 (C_{bpy}), 113.57 (-C≡**C**-bpy), 108.00 (-C≡**C**-DTE), 31.45 (m, ($P(CH_2CH_2)P$), 14.59 ($Me_{1'}$), 14.48 (Me_1). The assignment is based on 2D NMR studies. The carbon bearing fluorine or directly linked to ruthenium are not observed. FT-IR (cm^{-1}, ATR) = 2048, υ(C≡C). HR-MS EI: *m/z* 1545.2801 $[M+H]^+$, Calculated ($C_{87}H_{69}N_2F_6P_4S_2Ru$) 1545.2794. Elem. Anal. Calcd for $C_{87}H_{68}N_2F_6P_4S_2Ru$: C, 60.08; H, 4.15; N, 1.56; S, 3.56; Found C, 60.09; H, 4.47; N, 1.66; S, 3.50.

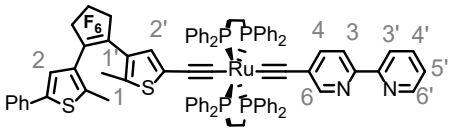

1o

***trans*-[Ph-DTE-C≡C-(dppe)$_2$Ru-C≡C-bipy-Yb(TTA)$_3$] 2o.** In a Schlenk tube, $Yb(TTA)_3,2H_2O$ (47.4 mg, 0.054 mmol) and **1o** (80 mg, 0.054 mmol) were dried under vacuum for 30 min. Then, the solids were dissolved in dichloromethane (30 mL). The solution was stirred at ambient temperature for 16 hours. The color of the solution changed from green to greenish yellow. The mixture was then taken to dryness under vacuum. The complex was precipitated by addition of pentane in dichloromethane solution to yield greenish yellow crystals (103 mg, 80 %). ^{1}H NMR ($CDCl_3$, 500 MHz): δ (ppm) = -10.90 (s, 3H, H_A TTA), 1.89 (s, 3H, Me), 2.01 (s, 3H, Me), 2.52 (s, 4H, $P(CH_2)_2P$), 2.79 (s, 4H, $P(CH_2)_2P$), 5.28 (s, 3H, TTA), 6.43 (s, 1H, $H_{2'}$), 6.62 (s, 3H, TTA) 6.73 (bs, 12H, m-PPh_2 and p-PPh_2), 6.98-7.01 (m, 8H, m-PPh_2), 7.17-7.20 (m, 4H, p-PPh_2), 7.33 (s, 1H, H_2), 7.39-7.42 (m, 2H, C_6H_5-DTE), 7.57-7.59 (m, 11H, o-PPh_2 and C_6H_5-DTE), 7.67 (m, 8H, o-PPh_2), 7.84 (s, 3H, TTA), 13.09 (s, 1H, H_{bpy}), 13.62 (s, 1H, H_{bpy}), 15.30 (s, 1H, H_{bpy}), 19.4 (s, 1H, H_{bpy}) 21.44 (s, 1H, H_{bpy}), 22.48 (s, 1H, H_{bpy}), 26.5 (bs, 1H, H_{bpy}). ^{31}P NMR ($CDCl_3$, 400 MHz): δ (ppm) = 52.82 (s, 4P). FT-IR (cm^{-1}, ATR) = 2039, υ(C≡C), 1600 υ(C=O), 1184 υ(C-F). HR-MS ESI ($CHCl_3$): *m/z* 2381.1740 $[M]^{+\cdot}$, Calculated ($C_{111}H_{80}N_2O_6F_{15}P_4S_5RuYb$) 2381.17577. Elem. Anal. Calcd for $C_{111}H_{80}N_2O_6F_{15}P_4S_5RuYb.CH_2Cl_2$: C, 54.55; H, 3.35; N, 1.14; S, 6.50; Found C, 54.15; H, 3.24; N, 0.97; S, 6.17.

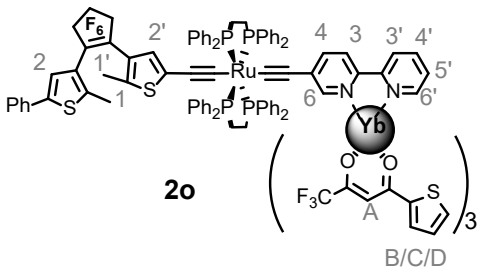

2o

B/C/D

ASSOCIATED CONTENT

Supporting Information

The Supporting Information is available free of charge on the ACS Publications website.

Details of spectroscopic measurements and DFT calculations are provided as supporting information (PDF)

AUTHOR INFORMATION

Corresponding Author

* e-mail addresses : lucie.norel@univ-rennes1.fr, stephane.rigaut@univ-rennes1.fr .

ACKNOWLEDGMENT

We thank the Université de Rennes 1, the CNRS, the ANR (RuOx-Lux - ANR-12-BS07-0010-01) and MESR for support. This work was performed using HPC/AI resources from GENCI-[CINES/TGCC] (Grant 2020-AP010811752 and 2021-AP0090811914).

REFERENCES

(1) *Molecular Switches*. Wiley-VCH, Weinheim, Germany: 2011.

(2) Pianowski, Z. L., Recent Implementations of Molecular Photoswitches into Smart Materials and Biological Systems. *Chemistry – A European Journal* **2019,** *25* (20), 5128-5144.

(3) Feringa, B. L., Vision Statement: Materials in Motion. *Adv. Mater.* **2020,** *32* (20), 1906416.

(4) Irie, M.; Fulcaminato, T.; Matsuda, K.; Kobatake, S., Photochromism of Diarylethene Molecules and Crystals: Memories, Switches, and Actuators. *Chem. Rev.* **2014,** *114* (24), 12174-12277.

(5) Zhang, J.; Tian, H., The Endeavor of Diarylethenes: New Structures, High Performance, and Bright Future. *Advanced Optical Materials* **2018,** *6* (6), 1701278.

(6) Goulet-Hanssens, A.; Eisenreich, F.; Hecht, S., Enlightening Materials with Photoswitches. *Adv. Mater.* **2020,** *32* (20), 1905966.

(7) Tian, Z.; Li, A. D. Q., Photoswitching-Enabled Novel Optical Imaging: Innovative Solutions for Real-World Challenges in Fluorescence Detections. *Acc. Chem. Res.* **2013,** *46* (2), 269-279.

(8) Abdollahi, A.; Roghani-Mamaqani, H.; Razavi, B.; Salami-Kalajahi, M., Photoluminescent and Chromic Nanomaterials for Anticounterfeiting Technologies: Recent Advances and Future Challenges. *ACS Nano* **2020**.

(9) Natali, M.; Giordani, S., Molecular switches as photocontrollable "smart" receptors. *Chem. Soc. Rev.* **2012,** *41* (10), 4010-4029.

(10) Hasegawa, Y.; Nakagawa, T.; Kawai, T., Recent progress of luminescent metal complexes with photochromic units. *Coord. Chem. Rev.* **2010,** *254* (21-22), 2643-2651.

(11) Galangau, O.; Norel, L.; Rigaut, S., Metal complexes bearing photochromic ligands: photocontrol of functions and processes. *Dalton Trans* **2021,** *50* (48), 17879-17891.

(12) Wang, J.-X.; Li, C.; Tian, H., Energy manipulation and metal-assisted photochromism in photochromic metal complex. *Coord. Chem. Rev.* **2021,** *427*.

(13) Eliseeva, S. V.; Bunzli, J.-C. G., Lanthanide luminescence for functional materials and bio-sciences. *Chem. Soc. Rev.* **2010,** *39* (1), 189-227.

(14) Bünzli, J.-C. G., On the design of highly luminescent lanthanide complexes. *Coord. Chem. Rev.* **2015,** *293-294*, 19-47.

(15) Wang, N.; Wang, J.; Zhao, D.; Mellerup, S. K.; Peng, T.; Wang, H.; Wang, S., Lanthanide Complexes with Photochromic Organoboron Ligand: Synthesis and Luminescence Study. *Inorg. Chem.* **2018,** *57* (16), 10040-10049.

(16) Nakagawa, T.; Atsumi, K.; Nakashima, T.; Hasegawa, Y.; Kawai, T., Reversible luminescence modulation in photochromic europium(III) complex having triangle terthiazole ligands. *Chem. Lett.* **2007,** *36* (3), 372-373.

(17) Nakagawa, T.; Hasegawa, Y.; Kawai, T., Photoresponsive europium(III) complex based on photochromic reaction. *J. Phys. Chem. A* **2008,** *112* (23), 5096-5103.

(18) Nakagawa, T.; Hasegawa, Y.; Kawai, T., Nondestructive luminescence intensity readout of a photochromic lanthanide(III) complex. *Chem. Commun.* **2009,** (37), 5630-5632.

(19) Cheng, H.-B.; Zhang, H.-Y.; Liu, Y., Dual-Stimulus Luminescent Lanthanide Molecular Switch Based on an Unsymmetrical Diarylperfluorocyclopentene. *J. Am. Chem. Soc.* **2013,** *135* (28), 10190-10193.

(20) Cheng, H. B.; Hu, G. F.; Zhang, Z. H.; Gao, L.; Gao, X.; Wu, H. C., Photocontrolled Reversible Luminescent Lanthanide Molecular Switch Based on a Diarylethene-Europium Dyad. *Inorg. Chem.* **2016,** *55* (16), 7962-8.

(21) Mei, J. F.; Lv, Z. P.; Lai, J. C.; Jia, X. Y.; Li, C. H.; Zuo, J. L.; You, X. Z., A novel photo-responsive europium(III) complex for advanced anti-counterfeiting and encryption. *Dalton Trans.* **2016,** *45* (13), 5451-5454.

(22) Koji, M.; Yoshio, N.; Keiichi, K., Photochemical Modulation of Europium Ion Fluorescence Using a Tetraazamacrocyclic Derivative Bearing a Spirobenzopyran and Three Carboxymethyl Moieties. *Bull. Chem. Soc. Jpn.* **2009,** *82* (4), 472-474.

(23) Hu, F.; Li, X.; Leng, Y.; Zhang, Y.; Zhou, M.; Ou, Y., Luminescent switch: Synthesis, characterization, and properties of some europium-based dithienylethenes. *Inorg. Chim. Acta* **2017,** *458*, 45-49.

(24) Li, Z.-Y.; Dai, J.-W.; Damjanović, M.; Shiga, T.; Wang, J.-H.; Zhao, J.; Oshio, H.; Yamashita, M.; Bu, X.-H., Structure Switching and Modulation of the Magnetic Properties in Diarylethene-Bridged Metallosupramolecular Compounds by Controlled Coordination-Driven Self-Assembly. *Angew. Chem. Int. Ed.* **2019,** *58* (13), 4339-4344.

(25) Zhou, Y.; Zhang, H.-Y.; Zhang, Z.-Y.; Liu, Y., Tunable Luminescent Lanthanide Supramolecular Assembly Based on Photoreaction of Anthracene. *J. Am. Chem. Soc.* **2017,** *139* (21), 7168-7171.

(26) He, X.; Norel, L.; Hervault, Y.-M.; Métivier, R.; D'Aléo, A.; Maury, O.; Rigaut, S., Modulation of Eu(III) and Yb(III) Luminescence Using a DTE Photochromic Ligand. *Inorg. Chem.* **2016,** *55* (24), 12635-12643.

(27) Zhang, Y.; Zhou, Y.; Gao, T.; Yan, P.; Li, H., Metal-directed synthesis of quadruple-stranded helical Eu(III) molecular switch: a significant improvement in photocyclization quantum yield. *Chem Commun (Camb)* **2020,** *56* (86), 13213-13216.

(28) Verma, P.; Singh, A.; Maji, T. K., Photo-modulated wide-spectrum chromism in Eu3+ and Eu3+/Tb3+ photochromic coordination polymer gels: application in decoding secret information. *Chem. Sci.* **2021,** *12* (7), 2674-2682.

(29) Norel, L.; Galangau, O.; Al Sabea, H.; Rigaut, S., Remote Control of Near Infrared Emission with Lanthanide Complexes. *ChemPhotoChem* **2021,** *5* (5), 393-405.

(30) Al Sabea, H.; Norel, L.; Galangau, O.; Roisnel, T.; Maury, O.; Riobé, F.; Rigaut, S., Efficient Photomodulation of Visible Eu (III) and Invisible Yb (III) Luminescences using DTE Photochromic Ligands for Optical Encryption. *Adv. Funct. Mater.* **2020**, 2002943.

(31) Di Piazza, E.; Norel, L.; Costuas, K.; Bourdolle, A.; Maury, O.; Rigaut, S., d-f Heterobimetallic Association between Ytterbium and Ruthenium Carbon-Rich Complexes: Redox Commutation of Near-IR Luminescence. *J. Am. Chem. Soc.* **2011,** *133* (16), 6174-6176.

(32) Al Sabea, H.; Norel, L.; Galangau, O.; Hijazi, H.; Métivier, R.; Roisnel, T.; Maury, O.; Bucher, C.; Riobé, F.; Rigaut, S., Dual Light and Redox Control of NIR Luminescence with Complementary Photochromic and Organometallic Antennae. *J. Am. Chem. Soc.* **2019,** *141* (51), 20026-20030.

(33) Al Sabea, H.; Hamon, N.; Galangau, O.; Norel, L.; Maury, O.; Riobé, F.; Tripier, R.; Rigaut, S., Efficient luminescence control in dithienylethene functionalized cyclen macrocyclic lanthanide complexes. *Inorg. Chem. Front.* **2020,** *7* (16), 2979-2989.

(34) Jukes, R. T. F.; Adamo, V.; Hartl, F.; Belser, P.; De Cola, L., Photochromic dithienylethene derivatives containing Ru(II) or Os(II) metal units. Sensitized photocyclization from a triplet state. *Inorg. Chem.* **2004,** *43* (9), 2779-2792.

(35) Ko, C. C.; Kwok, W. M.; Yam, V. W.; Phillips, D. L., Triplet MLCT photosensitization of the ring-closing reaction of diarylethenes by design and synthesis of a photochromic rhenium(I) complex of a diarylethene-containing 1,10-phenanthroline ligand. *Chemistry* **2006,** *12* (22), 5840-8.

(36) Roberts, M. N.; Nagle, J. K.; Finden, J. G.; Branda, N. R.; Wolf, M. O., Linker-dependent metal-sensitized photoswitching of dithienylethenes. *Inorg. Chem.* **2009,** *48* (1), 19-21.

(37) Roberts, M. N.; Nagle, J. K.; Majewski, M. B.; Finden, J. G.; Branda, N. R.; Wolf, M. O., Charge transfer and intraligand excited state interactions in platinum-sensitized dithienylethenes. *Inorg. Chem.* **2011,** *50* (11), 4956-66.

(38) Guerchais, V.; Ordronneau, L.; Le Bozec, H., Recent developments in the field of metal complexes containing photochromic ligands: Modulation of linear and nonlinear optical properties. *Coord. Chem. Rev.* **2010,** *254* (21), 2533-2545.

(39) Roke, D.; Stuckhardt, C.; Danowski, W.; Wezenberg, S. J.; Feringa, B. L., Light-Gated Rotation in a Molecular Motor Functionalized with a Dithienylethene Switch. *Angew. Chem. Int. Ed.* **2018,** *57* (33), 10515-10519.

(40) Grosshenny, V.; Romero, F. M.; Ziessel, R., Construction of Preorganized Polytopic Ligands via Palladium-Promoted Cross-Coupling Reactions. *J. Org. Chem.* **1997,** *62* (5), 1491-1500.

(41) Costuas, K.; Rigaut, S., Polynuclear carbon-rich organometallic complexes: clarification of the role of the bridging ligand in the redox properties. *Dalton Trans.* **2011,** *40* (21), 5643-5658.

(42) Norel, L.; Di Piazza, E.; Feng, M.; Vacher, A.; He, X. Y.; Roisnel, T.; Maury, O.; Rigaut, S., Lanthanide Sensitization with Ruthenium Carbon-Rich Complexes and Redox Commutation of Near-IR Luminescence. *Organometallics* **2014,** *33* (18), 4824-4835.

(43) Bourdolle, A.; Allali, M.; D'Aleo, A.; Baldeck, P. L.; Kamada, K.; Williams, J. A. G.; Le Bozec, H.; Andraud, C.; Maury, O., Influence of the Metal Ion on the Two-Photon Absorption Properties of Lanthanide Complexes Including Near-IR Emitters. *Chemphyschem* **2013,** *14* (14), 3361-3367.

(44) Pointillart, F.; Le Guennic, B.; Maury, O.; Golhen, S.; Cador, O.; Ouahab, L., Lanthanide Dinuclear Complexes Involving Tetrathiafulvalene-3-pyridine-N-oxide Ligand: Semiconductor Radical Salt, Magnetic, and Photophysical Studies. *Inorg. Chem.* **2013,** *52* (3), 1398-1408.

(45) Li, B.; Wang, J.-Y.; Wen, H.-M.; Shi, L.-X.; Chen, Z.-N., Redox-Modulated Stepwise Photochromism in a Ruthenium Complex with Dual Dithienylethene-Acetylides. *J. Am. Chem. Soc.* **2012,** *134* (38), 16059-16067.

(46) Wen, H.-M.; Li, B.; Wang, J.-Y.; Shi, L.-X.; Chen, C.-N.; Chen, Z.-N., Multistate Photochromism in a Ruthenium Complex with Dithienylethene–Acetylide. *Organometallics* **2013,** *32* (6), 1759-1765.

For table of Content Only

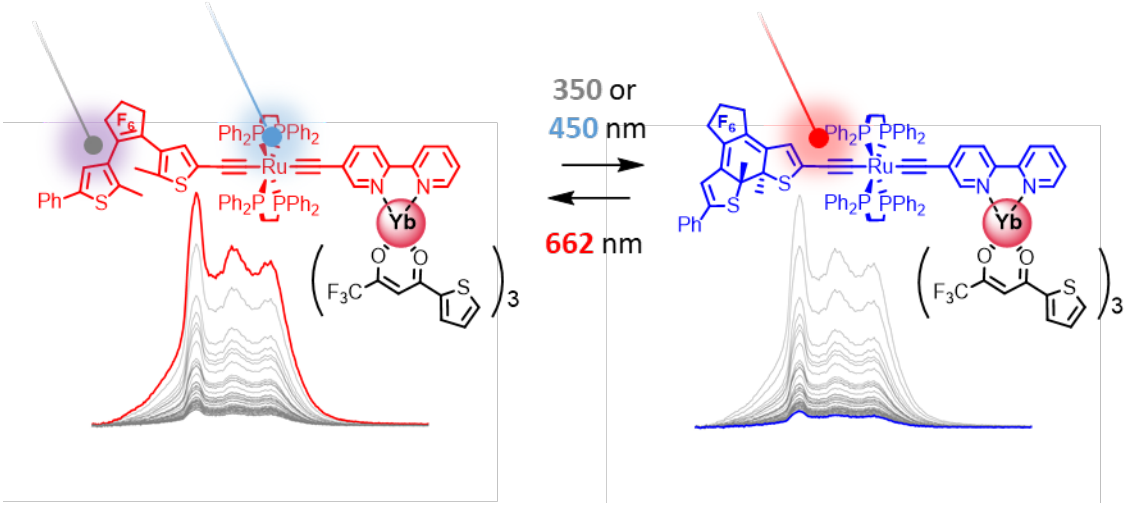

A unique combination of an emissive ytterbium(III) center with a photochromic ruthenium bisacetylide moiety provides a light and redox sensitive bimetallic complex. The high degree of electronic coupling between the diarylethene moiety and the rest of the ruthenium bisacetylide, evidenced through DFT calculations, leads to visible light induced isomerization reaction to the closed state. Therefore, the ytterbium centered NIR emission can be switched ON and OFF with visible light only, ie. using 450 nm and 662 nm irradiation wavelengths, therefore allowing the use of low energy excitations in both directions.